Experimental verification of Förster energy transfer between semiconductor quantum dots

DaeGwi Kim,* Shinya Okahara, and Masaaki Nakayama
Department of Applied Physics, Osaka City University, 3-3-138 Sugimoto, Sumiyoshi-ku, Osaka 558-8585, Japan

YongGu Shim
Department of Physics and Electronics, Osaka Prefecture University, 1-1 Gakuen-cho, Naka-ku, Sakai, Osaka 599-8531, Japan
(Received 16 June 2008; revised manuscript received 4 August 2008; published 2 October 2008)

In recent years, energy transfer (ET) using semiconductor quantum dots (QDs) is getting increased attention. However, it has been postulated that ET between QDs is based on the Förster model, which is a well-established model of ET mechanism in organic dye systems, without verification. In this work, we have investigated ET mechanism in colloidal CdS QDs measuring photoluminescence dynamics of a bilayer structure consisting of differently sized CdS QDs. In the bilayer structure, the distance between the monolayer of donor QDs and that of acceptor QDs was controlled precisely by a spacer layer that is layer-by-layer assembly of polyelectrolytes. The bilayer structure enabled us to systematically measure the spacer-layer dependence of photoluminescence dynamics reflecting the ET process between QDs. It is demonstrated that ET between the donor and acceptor QDs is conclusively dominated by the dipole-dipole interaction, which verifies the appropriateness of the Förster model.

DOI: 10.1103/PhysRevB.78.153301 PACS number(s): 78.67.Hc, 78.55.Et

Since the first report of quantum size effects in semiconductor doped glasses[1] and also in colloidal solutions[2] in the early 1980s, semiconductor quantum dots (QDs) have attracted considerable attention. So far, many studies have been conducted from a scientific viewpoint to understand the intrinsic nature of physical/chemical properties of QDs, as well as from interest in the application to new functional materials.[3–6] A turning point in QD studies was the development of monodispersed colloidal QDs having high photoluminescence (PL) yield with use of rapid injection of organometallic precursors into hot coordinating solvents (hot-injection method).[7,8] The breakthrough in synthesizing the new class of colloidal QDs have led to an explosive increase in QD studies and opened up possibilities for various applications such as biomolecular imaging,[9] QD lasing,[6,10] and QD solar cells.[11,12]

Randomly dispersed QDs have been a major target in most of the studies so far. The dynamical process of resonant ET between CdSe QDs was reported in recent years.[13,14] This opened up a new aspect in photophysics of semiconductor QDs and stimulated studies on QD-based energy transfer (ET) processes employing QDs as energy donors in QD-bioconjugate systems[9] and QD-organic dye systems,[15,16] as well as ET between QDs.[17,18] All of the studies, however, have postulated that ET employing QDs is based on the Förster model[19] that is a typical ET mechanism between organic molecules. It should be noted that the appropriateness of the Förster model for explanation of ET in QDs has not been verified until now. For the experimental clarification of the ET mechanism, it is essential to measure PL dynamics in a well-designed sample structure in which the distance between QDs was precisely controlled.

How can we control the distance between QDs? We have focused on a layer-by-layer (LBL) assembly.[20–22] LBL is a simple and powerful technique allowing the realization of a multilayer structure that is controlled at a molecular level. This technique is based on the sequential adsorption of oppositely charged species and has been most widely used to assemble various types of polymers. A successful preparation of multilayer structures of semiconductor QDs such as CdTe,[23] CdS,[24] and CdSe[25] using the LBL assembly technique was reported so far. In the present work, we employed the LBL assembly technique to realize ET between colloidal CdS QDs and to control it. As shown in Fig. 1, we fabricated bilayer structures consisting of differently sized CdS QDs, which is a similar structure reported by Klimov and coworkers.[14] In this structure, efficient "vertical" ET from smaller QDs to larger QDs is realized like a donor-acceptor system.

Our key idea is that the distance between two QD monolayers in the bilayer structure can be controlled by the spacer-layer thickness with nanometer accuracy by using LBL assembly of oppositely charged polyelectrolytes (Fig. 1). The spacer layer was deposited by LBL assembly of positively charged poly(diallyldimethylammonium chloride) (PDDA) and negatively charged poly(acrylic acid) (PAA).

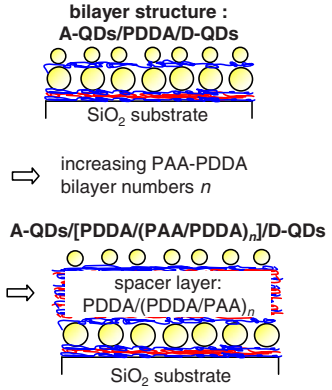

FIG. 1. (Color online) Schematic diagram of the deposition process of the bilayer structure. The bilayer structure consisting of a monolayer of energy-donor QDs (A-QDs), followed by a "spacer layer" of polyelectrolytes, and a monolayer of energy-donor QDs (D-QDs). The spacer-layer thickness is controlled by the number of PAA/PDDA bilayers *n*. The energy transfer can be controlled by the spacer-layer thickness.

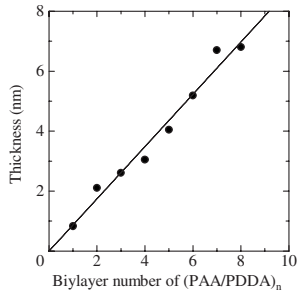

FIG. 2. The thickness of PAA/PDDA bilayers, which was determined by spectroscopic ellipsometry, as a function of n. The solid line denotes the analysis with least-squares fitting; the average thickness of one bilayer of PDDA/PAA can be estimated to be 0.9 nm.

The thickness of the spacer layer was controlled by number of PAA-PDDA bilayers.

In this paper, we study the ET mechanism in CdS QDs measuring the dependence of PL dynamics on the spacer-layer thickness. It is demonstrated that ET between the donor and acceptor QDs is conclusively dominated by the dipole-dipole interaction, which verifies the appropriateness of the Förster model.

In the beginning of the sample preparation, adhesion layers of $PDDA/(PAA/PDDA)_2$ were deposited to enhance the

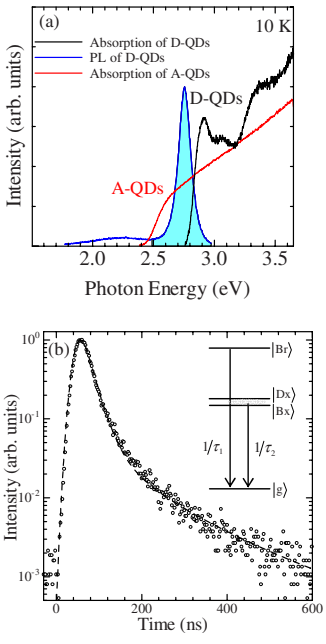

FIG. 3. (Color online) (a) Absorption and PL spectra at 10 K of D-QDs of CdS dispersed in PVA films. The spectral overlap of the band-edge PL of the D-QDs with the absorption of the A-QDs is fully realized, which assures effective ET from the D-QDs to the A-QDs in the bilayer structure. (b) PL-decay profiles of the D-QDs at 10 K. The broken curve denotes the results of the convolution analysis between the laser pulse profile with the Gaussian function and the PL-decay function of Eq. (1). Inset: Schematics of emitting transitions in CdS QDs from the bright exciton state ($|\mathrm{Br}\rangle$) with the decay time of τ_1 and from the dark exciton state ($|\mathrm{Dx}\rangle$) and the lower-lying bound-exciton state ($|\mathrm{Bx}\rangle$) in quasithermal equilibrium with the decay time of τ_2 (Ref. 27).

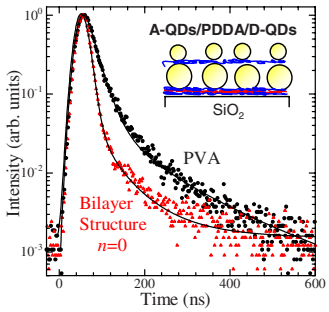

FIG. 4. (Color online) PL-decay profiles of the D-QDs of CdS in the bilayer structures of A-QDs/PDDA/D-QDs. Triangles and circles represent PL-decay profiles of the D-QDs in the bilayer structures and in the PVA film, respectively. Solid curves are the results of the decay profile analysis.

binding of the bilayer structure of CdS QDs to SiO_2 substrates. Then, the bilayer structures were composed of three main blocks: the monolayer of larger QDs, which acts as energy-acceptor QDs (A-QDs), followed by the spacer layer of $PDDA/(PAA/PDDA)_n$, where the notation of $(PAA/PDDA)_n$ represents the n bilayers of PAA and PDDA, and the monolayer of smaller QDs as energy-donor QDs (D-QDs): $A\text{-}QDs/[PDDA/(PAA/PDDA)_n]/D\text{-}QDs$ (Fig. 1).[26]

The A-QDs of CdS with a diameter of 5.0 nm were synthesized by a colloidal method as reported in Ref. 27. The D-QDs of CdS were prepared by a combination of a size-selective photoetching and a surface modification technique with a $Cd(OH)_2$ layer,[27,28] which enabled us to prepare size-controlled CdS QDs with high PL efficiency. We prepared bilayer structures using differently sized D-QDs with diameters of 4.2, 4.4, 4.5, and 4.7 nm and A-QDs with a diameter of 5.0 nm.

Spectroscopic ellipsometry was adopted to determine an accurate thickness of the polymer. The measurements were performed by a spectroscopic phase modulated ellipsometer in the spectral range from 1.5 eV to 4.0 eV. For measurements of PL-decay profiles, third-harmonic-generation light (355 nm) of a laser-diode pumped yttrium aluminum garnet laser with a repetition of 10 kHz was used as the excitation light. The pump fluence was 3 $\mu J/cm^2$, exciting <0.01 excitons per dot on average. The PL-decay profiles were detected with a streak-camera system. The time resolution of our system was estimated to be ~ 4.7 ns from the analysis of a laser pulse profile with a Gaussian function of $\exp(-t^2/2w^2)$, where the width w corresponds to the time resolution. In order to determine the PL-decay time, the PL-decay profiles have been fitted using a convolution between the laser excitation and the PL-decay function.

Figure 2 shows the total layer thickness of PAA/PDDA LBL films, which was determined by spectroscopic ellipsometry, as a function of the number of bilayers n. A linear dependence of the layer thickness on n is clearly observed; therefore, the average thickness of one bilayer of PAA/PDDA can be estimated to be 0.9 nm from least-squares fitting (solid line). Thus, it is expected that the distance between the QD layers in the bilayer structure can be controlled with the accuracy of 0.9 nm.

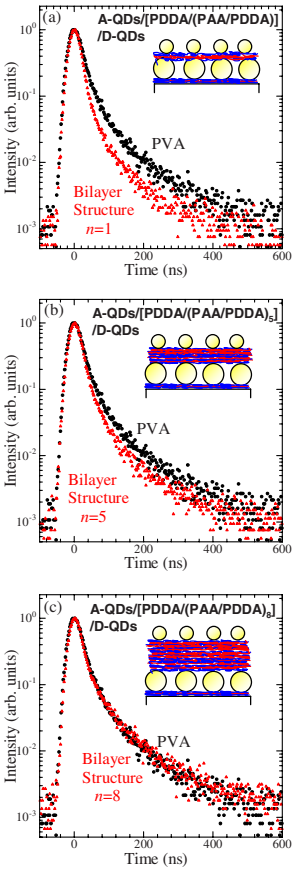

FIG. 5. (Color online) PL-decay profiles of the D-QDs of CdS in the bilayer structures of A-QDs/[PDDA/(PAA/PDDA)$_n$]/D-QDs with different numbers of PAA-PDDA bilayers; (a) $n=1$, (b) $n=5$, and (c) $n=8$. Triangles and circles represent PL-decay profiles of the D-QDs in the bilayer structure and in the PVA film, respectively.

Before discussion for PL dynamics of the bilayer structure, we first discuss PL properties of D-QDs which were dispersed in a polyvinyl alcohol (PVA) film as a control sample. Since a mean distance between QDs in the PVA film is more than 50 nm due to a dilute concentration of QDs,[29] ET between QDs can be ignored. Figure 3(a) shows absorption and PL spectra at 10 K of the D-QDs of CdS dispersed in the PVA film. The absorption peaks, which originate from the ground state and from the higher excited states of excitons in the CdS QDs, are observed clearly. In the PL spectrum, the band-edge PL is observed as a main PL band. These results indicate the successful preparation of the size- and surface-controlled QDs, which enabled us to observe the precise spacer-layer-thickness dependence of PL dynamics of the D-QDs. It is noted that the spectral overlap between the band-edge PL of the D-QDs and the absorption of the A-QDs is fully realized as shown in Fig. 3(a), which assures effective ET from the D-QDs to the A-QDs in the bilayer structure.

Figure 3(b) shows the PL-decay profiles of the D-QDs of CdS in the PVA film at 10 K. The detection energy was 2.66 eV. It is noted that the decay profiles of the D-QDs in the PVA film do not depend on the detection energy. The decay profile can be explained quantitatively by a combination of

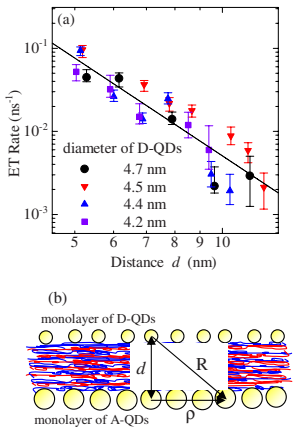

FIG. 6. (Color online) The dependence of k_{ET} on the distance between D-QDs and A-QDs is shown in (a). In the bilayer structure studied in the present work, all of the ET process from the D-QDs to the A-QDs in the layered structure should be considered as in (b).

one monoexponential and one stretched exponential functions:[27]

$$A_1 \exp(-t/\tau_1) + A_2 \exp[-(t/\tau_2)^{\beta}], \quad (1)$$

where τ_1 is the decay time of the bright exciton state $|\mathrm{Br}\rangle$, and τ_2 corresponds to the decay time that is characterized by the dark exciton state $|\mathrm{Dx}\rangle$ and bound-exciton state $|\mathrm{Bx}\rangle$ in quasithermal equilibrium.[27] The energy scheme is shown in the inset of Fig. 3(b). In order to estimate the decay time, the PL-decay profiles have been fitted using the convolution between the laser pulse profile with the Gaussian function and the PL-decay function of Eq. (1). The broken curve denotes the results of the convolution analysis.

Hereafter, we discuss the PL dynamics in the bilayer structure. Figure 4 shows the PL-decay profile of the D-QDs in the bilayer structure of A-QDs/PDDA/D-QDs. The detection energy was 2.66 eV. In contrast to the PVA film sample, the decay profiles in the monolayer structure of the D-QDs depend on the detection energy, and the higher-energy component in the PL band exhibits a faster decay as compared with the PVA film sample. The shortened decay time at higher detection energy originates from ET between nearby QDs in the single monolayer of the D-QDs. In order to eliminate the contribution of in-plane ET process in the monolayer of the D-QDs, the PL-decay profiles were detected at 2.66 eV that is lower than the absorption onset energy. We note that the decay profile detected at 2.66 eV in the monolayer of the D-QDs corresponds to that in the PVA film, indicating full suppression of the in-plane ET process.

The decay profile in the bilayer structure is faster than that in the PVA film sample, where the decay profile of the D-QDs in the PVA film, in which ET between QDs can be ignored, is depicted by circles for comparison in Fig. 4. This result obviously shows the occurrence of direct ET from the D-QDs to the A-QDs in the bilayer structure. The solid curves depict fitting results by the convolution. A notable change of τ_1 is observed; 20 ns in the PVA film and 7 ns in the bilayer structure. Thus, ET from the bright exciton state $|\mathrm{Br}\rangle$ in the D-CdS QDs is considered to be dominant, which

is similar to the results reported for CdSe and CdTe QDs.[14,17] The energy-transfer rate (k_{ET}) in the bilayer structure can be estimated to be 0.09 ns^{-1} from the following expression: $k_{ET}=(1/\tau_{PVA}-1/\tau_{bilayer})^{-1}$, where τ_{PVA} and $\tau_{bilayer}$ are the decay time of the bright exciton state in the PVA film sample and that in the bilayer structure, respectively.

The decay profiles in the bilayer structures with $n=1$ and $n=5$ of $(PAA/PDDA)_n$ spacer layer are faster than that in the PVA film sample and become slower with increasing n as shown in Figs. 5(a) and 5(b). These results demonstrate that the ET rate from the D-QDs to the A-QDs becomes smaller with increasing spacer-layer thickness. Then, the decay profile in the bilayer structure with $n=8$ is consistent with that in the PVA film sample, indicating full suppression of the ET process [Fig. 5(c)]. The above results demonstrate a successful control of ET from the D-QDs to the A-QDs by changing the spacer-layer thickness with nanometer accuracy.

To reveal how k_{ET} depends on the distance between CdS QDs, we prepared bilayer structures using differently sized D-QDs with diameters of 4.2, 4.5, and 4.7 nm and A-QDs with a diameter of 5.0 nm. Then, the dependence of PL dynamics of the D-QDs on the spacer-layer thickness was systematically investigated. Figure 6(a) shows the dependence of k_{ET} on the distance between the D-QDs and the A-QDs. The "distance" (d) is defined as $d=R_D+L+R_A$, where R_D (R_A) denotes the radius of the D-QDs (A-QDs) and L the thickness of the spacer layer. The solid line is the result of the distance dependence of k_{ET} analyzed with the least-squares method. From the analysis, it is found that k_{ET} is proportional to $1/d^{3.9}$.

It is well known that the Förster ET rate (k_{ET}^F) is inversely proportional to R^6: $k_{ET}^F=C/R^6$, where R is the distance between two isolated dipoles (e.g., donor and acceptor molecules) and C the distance-independent factor. In the bilayer structure studied in the present work, QDs form a layered structure. Thus, the ET process from one D-QD to all the A-QDs in the layered structure should be considered as shown in Fig. 6(b); therefore, the Förster ET rate in this case is given by

$$k_{ET}=\sigma\int k_{ET}^F dS=\sigma C\int_0^\infty [2\pi\rho/(d^2+\rho^2)^3]d\rho, \qquad (2)$$

$$R^2=d^2+\rho^2,\ \ dS=2\pi\rho d\rho, \qquad (3)$$

where σ denotes the surface density of QDs in the layer of A-QDs. The d dependence of k_{ET} is obtained by performing integration of Eq. (2) as $k_{ET}\propto 1/d^4$. Thus, the almost fourth power dependence of k_{ET} on d can be quantitatively explained by the modified Förster model: namely, the dipole-dipole interaction dominates the ET process between QDs. As shown in Fig. 6(a), the data points of k_{ET} obtained in the bilayer structures employing four differently sized D-QDs exhibit the same distance dependence irrespective of the D-QD size. Thus, it is reasonable to define the "*distance*" between QDs as center-to-center spacing.

We have prepared bilayer structures of CdS QDs using LBL assembly in order to reveal the ET mechanism. The spacer-layer thickness between two monolayers of energy-donor QDs and energy-acceptor QDs was controlled with high accuracy of 0.9 nm. From the systematic study of the dependence of PL dynamics on the spacer-layer thickness, we have revealed that the ET mechanism between QDs is conclusively explained by the Förster model taking account of the bilayer structure.

This work was supported in part by a Grant-in-Aid for Scientific Research from JSPS and by JGC-S Scholarship Foundation.

*Present address: Department of Applied Physics, Osaka City University, 3-3-138 Sugimoto, Sumiyoshi-ku, Osaka 558-8585, Japan. tegi@a-phys.eng.osaka-cu.ac.jp

[1] A. I. Ekimov and A. A. Onushchenko, Sov. Phys. Semicond. **16**, 775 (1982).
[2] A. Henglein, Ber. Bunsenges. Phys. Chem. **86**, 301 (1982).
[3] U. Woggon, *Optical Properties of Semiconductor Quantum Dots* (Springer, New York, 1996).
[4] A. D. Yoffe, Adv. Phys. **50**, 1 (2001).
[5] Y. Masumoto and T. Takagahara, *Semiconductor Quantum Dots* (Springer, New York, 2002).
[6] V. I. Klimov, *Semiconductor and Metal Nanocrystals* (Dekker, New York, 2004).
[7] C. B. Murray *et al.*, J. Am. Chem. Soc. **115**, 8706 (1993).
[8] B. O. Dabbousi *et al.*, J. Phys. Chem. B **101**, 9463 (1997).
[9] I. L. Medintz *et al.*, Nature Mater. **4**, 435 (2005), and references therein.
[10] V. I. Klimov *et al.*, Science **290**, 314 (2000).
[11] A. J. Nozik, Physica E (Amsterdam) **14**, 115 (2002).
[12] I. Gur *et al.*, Science **310**, 462 (2005).
[13] C. R. Kagan *et al.*, Phys. Rev. B **54**, 8633 (1996).
[14] S. A. Crooker *et al.*, Phys. Rev. Lett. **89**, 186802 (2002).
[15] E. Alphandéry *et al.*, Chem. Phys. Lett. **388**, 100 (2004).
[16] S. Dayal and C. Burda, J. Am. Chem. Soc. **129**, 7977 (2007).
[17] T. Franzl *et al.*, Nano Lett. **4**, 1599 (2004).
[18] S. F. Wuister *et al.*, J. Phys. Chem. B **109**, 5504 (2005).
[19] T. Förster, Discuss. Faraday Soc. **27**, 7 (1959).
[20] G. Decher, Science **277**, 1232 (1997).
[21] G. Decher and J. B. Schlenoff, *Multilayer Thin Films: Sequential Assembly of Nanocomposite Materials* (Wiley, Weinheim, 2003).
[22] N. A. Kotov, *Nanoparticle Assemblies and Superstructures* (CRC, Boca Raton, FL, 2005).
[23] A. A. Mamedov *et al.*, J. Am. Chem. Soc. **123**, 7738 (2001).
[24] N. A. Kotov *et al.*, J. Phys. Chem. **99**, 13065 (1995).
[25] D. Zimnitsky *et al.*, Langmuir **23**, 4509 (2007).
[26] Recently, similar idea that LBL films of polyelectrolytes can be used as a spacer layer to control the distance between Au nanoparticles and CdTe QDs was reported; V. K. Komarala *et al.*, Appl. Phys. Lett. **89**, 253118 (2006).
[27] D. Kim *et al.*, J. Phys. Chem. C **112**, 10668 (2008).
[28] L. Spanhel *et al.*, J. Am. Chem. Soc. **109**, 5649 (1987).
[29] K. Tomihira *et al.*, J. Lumin. **122-123**, 471 (2007).